

# Characteristics of the Friction Between Aluminium and Steel at Elevated Temperatures During Ball-on-Disc Tests

Liliang Wang · Jingqi Cai · Jie Zhou ·  
Jurek Duszczek

Received: 25 March 2009 / Accepted: 17 June 2009 / Published online: 30 June 2009  
© The Author(s) 2009. This article is published with open access at Springerlink.com

**Abstract** Appropriate specification of the frictional boundary condition for the finite-element (FE) simulation of metal-forming processes is of great importance to the trustworthiness of the results. The research reported in this communication aimed at understanding the interfacial contact between aluminium and steel at elevated temperatures and determining friction coefficients at this material mating. A series of high-temperature ball-on-disc tests were carried out with the AA7475 aluminium alloy as the material of disc and the hardened H11 steel as the material of ball. A mathematical model developed in the preceding research was employed to account for the evolution of the contact interface during ball-on-disc tests. Friction coefficients at different temperatures and over a number of laps were determined. The shear friction stresses and mean contact pressures along with the progress of the tests at 350–500 °C were calculated. It was found that the friction coefficients obtained from ball-on-disc tests alone were insufficient to represent the frictional interaction between deforming aluminium and steel at elevated temperatures. The evolution of the contact interface with increasing sliding distance must be taken into consideration and the friction behaviour can be reasonably characterized by using friction stress.

**Keywords** Ball-on-disc test · FE Simulation · Extrusion · Friction coefficient

## 1 Introduction

Aluminium extrusion is a cost-efficient method for the mass production of rods, tubes and complexly shaped profiles [1–3]. The process involves highly complicated thermomechanical interactions within the workpiece and tribological reactions at the workpiece/tooling interfaces [4, 5]. In recent years, finite-element (FE) simulations have been increasingly used in scientific research and industrial practice to analyze the process and to aid in process optimization. Some of the simulation results are experimentally verifiable, which allows the fine-tuning of the input data and the redefinition of the boundary conditions for FE simulation. However, many other parameters, such as local temperatures, strains and stresses, are not experimentally measureable, such that there is a certain level of uncertainty about the input data, boundary conditions and thus the FE simulation results. In any case, correct definition of the deformation behaviour of the workpiece material, often expressed in the form of a constitutive equation, and appropriate specification of the frictional boundary conditions are of critical importance to the trustworthiness of the FE simulation results. A wealth of information on the deformability of aluminium alloys is available in the open literature. However, the nature of the friction during the aluminium extrusion process is far less well understood and, as a result, the rationale behind specifying certain friction boundary conditions at the billet/container interface and at the billet/die interface is often not clear.

Notwithstanding this, some efforts have been made to help with the selection of a suitable friction model and the

---

L. Wang (✉) · J. Zhou · J. Duszczek  
Department of Materials Science and Engineering,  
Delft University of Technology, Mekelweg 2, 2628 CD Delft,  
The Netherlands  
e-mail: liliang.wang@tudelft.nl

J. Cai  
Department of Mechanical Engineering, Imperial College  
London, London, UK

determination of a friction coefficient at the billet/container interface. The experimental approach was mostly taken to determine the friction coefficient at the billet/container interface from the difference in extrusion force due to a change in friction force at this interface during extrusion [6–8]. Using a similar approach, Flitta and Sheppard [9] revealed the dependence of friction coefficient at the billet/container interface on temperature during the aluminium extrusion process at elevated temperatures. A change in friction coefficient from essentially sliding friction to nearly sticking friction was found, when the billet temperature was increased from 300 to 450 °C. In addition, AA4043 (AlSi5.5) rod markers were inserted into the AA6060 billet to reveal the metal flow along the container wall and strong evidence was found that full sticking indeed occurred at the billet/container interface during extrusion [10].

The contact at the billet/die bearing interface where the extruded product is shaped is of vital importance for the product quality and die life. Preceding research using both the experimental approach and FE simulation [11–13] have shown that, being similar to the machining process [14], a transition from sticking to sliding takes place in the die bearing channel and thus the friction coefficients representing the change in friction mode must be incorporated into FE simulation. In addition, physical simulations, such as ring compression tests at room temperature [15] and block-on-disc tests at elevated temperatures [16] have been performed to characterize the tribological interactions between aluminium and steels. More recently, first attempts have been made to determine the friction coefficients between hot aluminium and steel by means of ball-on-disc tests during which conform contact between the deforming disc and ball is gradually established, which is closer to the actual contact at the die bearing during extrusion [17, 18].

Ball-on-disc test is one of the commonly used methods for characterizing the tribological properties of the

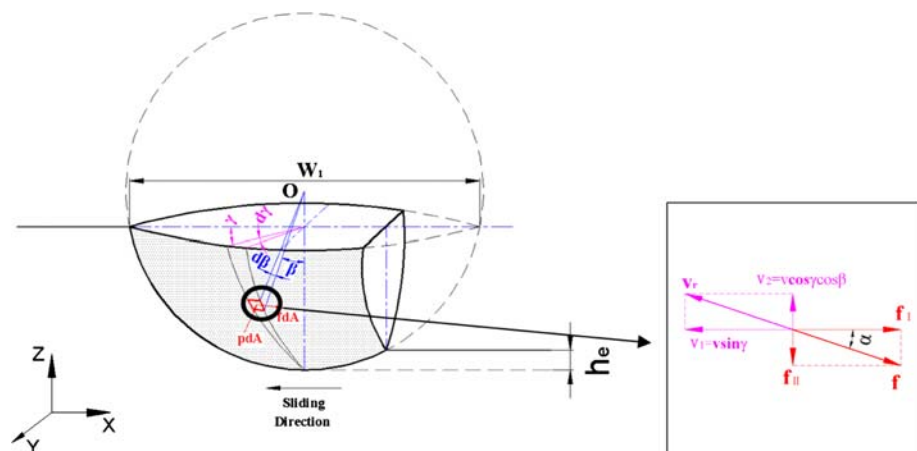
materials at contact. To authors' knowledge, the friction coefficients obtained from ball-on-disc tests have not yet been implemented in the FE simulation of aluminium extrusion, due to a lack of the methodology for translating the data from ball-on-disc tests to the extrusion process. As a comparison, the friction coefficients obtained from scratch tests with the plowing friction distinguished from the shear friction have recently been introduced into the FE simulation of the machining process [14]. Being different from scratch tests, during ball-on-disc tests, the ball slides over the same wear track repeatedly and, as a result, the contact differs greatly from one lap to another, due to the removal (wear) of the mating materials, especially during the tests at elevated temperatures. As a result of changing contact from one lap to another, the results obtained from ball-on-disc tests could not be utilized directly to specify the frictional boundary conditions for the FE simulations of aluminium extrusion. A fundamental understanding of the evolution of the contact interface between the ball and disc is of critical importance for correct interpretation of the results and then their translation to the contact at the billet/die bearing interface during aluminium extrusion.

In the preceding research, a model capable of revealing the features of the contact interface during high-temperature ball-on-disc tests and discriminating between the plowing friction and shear friction was developed [17]. The objective of the present research was to implement this model in practical contact situations between hot aluminium and H11 tool steel during ball-on-disc testing, and the results were expected to be extracted to define the frictional boundary condition for the FE simulation of the aluminium extrusion process.

## 2 Brief Model Description

Figure 1 shows the forces acting on an elemental area during ball-on-disc testing. These forces can be expressed

**Fig. 1** Close-up view of the friction force and velocity on an elemental area



by Eq. 1, which was developed on the basis of Tayebi’s model [19]:

$$\begin{cases} dF_x = \left( pr^2 \sin^2 \beta \cos \gamma + fr^2 \sin \beta \sqrt{\cos^2 \gamma \cos^2 \beta + \sin^2 \gamma} \right) d\gamma d\beta \\ dF_z = \left( pr^2 \cos \beta \sin \beta - fr^2 \frac{\cos \gamma \sin^2 \beta \cos \beta}{\sqrt{\cos^2 \gamma \cos^2 \beta + \sin^2 \gamma}} \right) d\gamma d\beta \end{cases} \quad (1)$$

### 2.1 First Lap of Wear

In the present work, the aluminium alloy AA7475 was used as the disc material, which was assumed to behave as a viscoplastic material at elevated temperatures and thus the elastic recovery of the disc at the rear part of the ball was omitted. During the first lap of wear, the contact interface was analogous to that during scratch tests. Figure 2 schematically shows the contact interface during the first lap of wear. Equation 2 can be used to calculate the tangential and normal forces acting on the ball surface:

$$\begin{cases} F_x = 2 \int_0^{\xi_1} \int_0^{\pi/2} dF_x \\ F_z = 2 \int_0^{\xi_1} \int_0^{\pi/2} dF_z \end{cases} \quad (2)$$

where  $\xi_1$  is the upper integral limit of angle  $\beta$  (see Fig. 2a where  $W_1$  is the width of the wear track after the first lap of wear).

### 2.2 Arbitrary (i + 1)th Lap of Wear

Being different from scratch tests, after the first lap of wear, some of the material in front of the ball was removed

during the preceding laps of sliding. The contact interface is schematically shown in Fig. 3. Equation 3 can be used to

calculate the tangential and normal forces acting on the ball:

$$\begin{cases} F_x = 2 \int_0^{f_i(\gamma)} \int_0^{\pi/2-\omega_i} dF_x + 2 \int_0^{\xi_i} \int_{\pi/2-\omega_i}^{\pi/2} dF_x \\ F_z = 2 \int_0^{f_i(\gamma)} \int_0^{\pi/2-\omega_i} dF_z + 2 \int_0^{\xi_i} \int_{\pi/2-\omega_i}^{\pi/2} dF_z \end{cases} \quad (3)$$

As shown in Fig. 3b, in the area  $COD$ ,  $f_i(\gamma)$  is the upper integral limit of  $\beta$ , and in the areas  $AOD$  and  $COB$ ,  $\xi_i$  is the upper integral limit of angle  $\beta$ .  $\omega_i$  is the angle for locating the position of the front contact boundary during the  $(i + 1)$ th lap of wear.

### 3 Materials and Experimental Procedure

In the present research, the high-strength AA7475 aluminium alloy disc had a thickness of 5 mm and a diameter of 49 mm. The surface of the disc with a hardness value of 53 HRA at room temperature was polished to an average roughness  $R_a$  of 33 nm. The H11 hot-work tool steel hardened to a hardness value of 53 HRC at room temperature was selected as the mating material. The ball had a diameter of 5 mm, and an average roughness of 209 nm.

**Fig. 2** Schematic drawing showing the contact interface in the first lap of wear during ball-on-disc testing

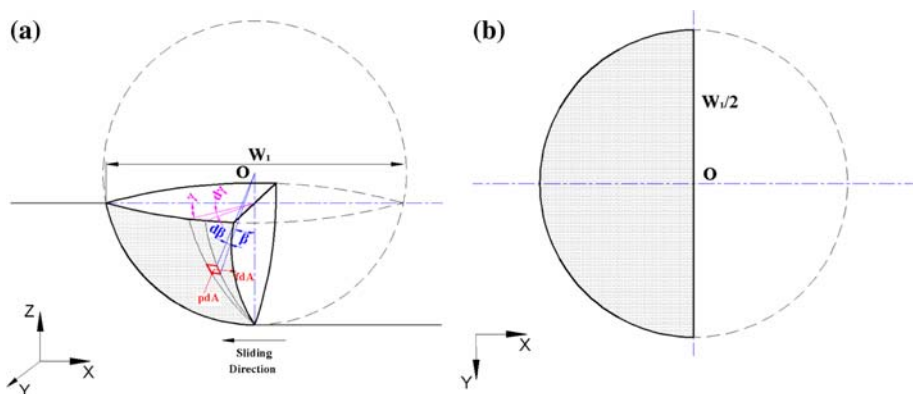


**Fig. 3** Schematic drawing showing the contact interface in an arbitrary ( $i + 1$ )th lap of wear during ball-on-disc testing

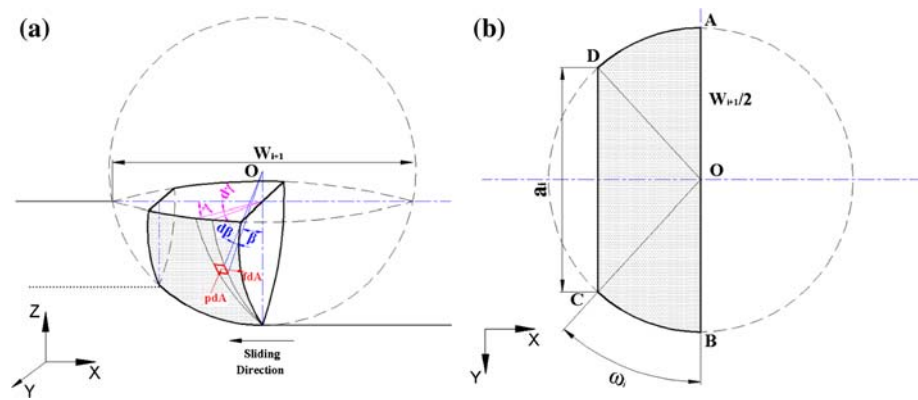


**Table 1** Compositions of H11 hot-work steel and AA7475 aluminium alloy (wt%)

H11 steel	C	Cr	Mn	Mo	Si	V	Fe		
	0.40	5.0	0.30	1.30	1.0	0.50	Balance		
AA7475	Si	Fe	Cu	Mn	Mg	Cr	Zn	Ti	Al
	0.10	0.12	1.9	0.06	2.4	0.18	5.2	0.06	Balance

The compositions of the materials used in the present research are given in Table 1.

A CSM<sup>®</sup> high-temperature tribometer with a ball-on-disc rig was used for a series of short-distance high-temperature friction tests in order to reach the solutions of the model developed. The radius of the wear track was 6 mm and the linear speed was 2 mm/s. The tests were carried out under a constant normal load of 6 N at 350, 400, 450 and 500 °C in the ambient atmosphere. Three tests with different wear laps (1, 5 and 10 laps) were carried out at each temperature. The short-distance tests under the relatively high normal load were desired to produce high contact pressures up to 120 MPa, which would resemble the situation in the bearing channel of the extrusion die during lab-scale extrusion experiments where the normal pressure varied from two to six times of the flow stress of the billet material. The friction coefficient was continuously registered during the test. Thereafter, wear tracks were examined using an optical microscope. The average width of the wear track in each lap was determined from 12 measurements.

## 4 Results and Discussion

### 4.1 Evolution of Friction Coefficient with Sliding Distance

Figure 4 shows the evolution of the friction coefficient over a sliding distance of 10 laps at different temperatures. It is of interest to note that friction coefficient increases with the sliding distance. At 500 °C, in particular, the

friction coefficient increases even by 50%. The significant variation of the friction coefficient with sliding distance during the ball-on-disc tests was also observed by other researchers [18], and this phenomenon was attributed to the material transfer and back transfer, which significantly altered the contact interface topography and changed the real contact area. However, in the present research, short distance friction tests (10 laps of sliding) were performed and the friction coefficients were found to increase steadily with the sliding distance, and thus the explanation [18] may not applicable. At the beginning stage of testing, the contact pressure was very high, and severe plastic deformation and drastic removal of surface material occurred. As shown below, the increase of friction coefficient with sliding distance appears to be accompanied by the increase in apparent contact area during the running-in period. Their correlation appears to be peculiar and occurs in the material mating at high temperatures with involvement of strong adhesion. The evolution of the friction coefficient with sliding distance, as shown in Fig. 4, leads to the uncertainty as to the exact value to be put into FE simulation. It is, therefore, necessary to have a model with which the friction coefficient and sliding distance are correlated with each other. In the present research, the friction coefficients and residual widths of wear tracks determined during and after the ball-on-disc tests were used as input data of the model, i.e. Eqs. 1–3. The evolutions of the contact area and shear friction stress were obtained.

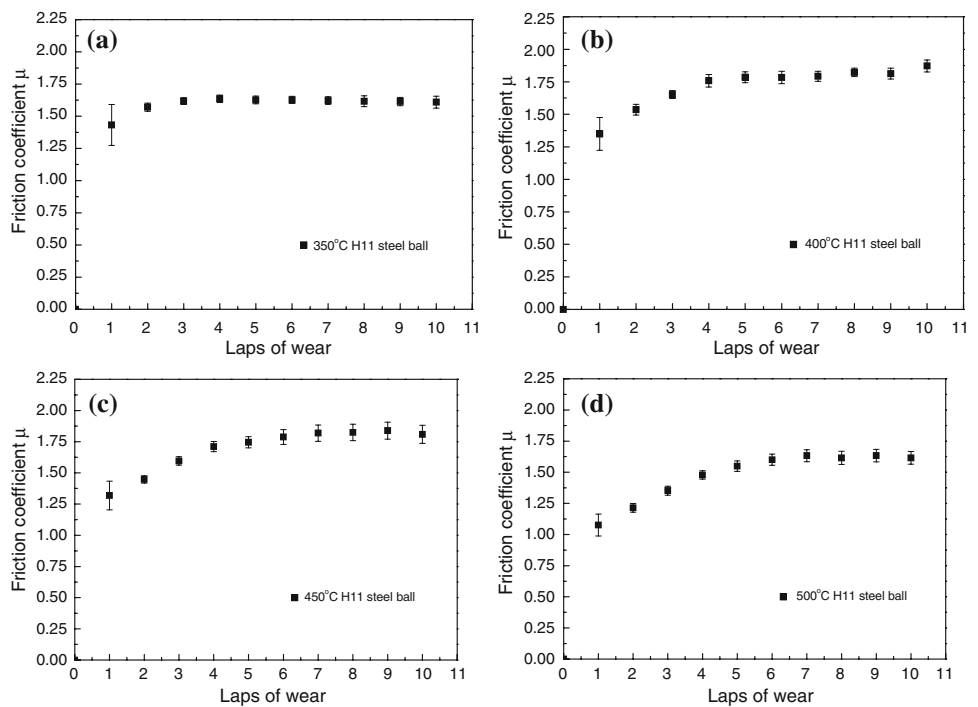
#### 4.1.1 Evolution of Wear Track Width

An average value of the widths of wear tracks was determined from 12 measurements by using an optical microscope. The residual width of the wear tracks can be fitted:

$$W_i = a \times i^b \quad (4)$$

where  $W_i$  is the width of the wear track after the  $i$ th lap of wear, and  $a$  and  $b$  are constants. Figure 5 shows the experimental and fitted results of the widths of wear tracks.

**Fig. 4** Evolution of the friction coefficient with increasing sliding distance at different temperatures



As can be seen, the widths of wear tracks increase steadily with increasing sliding distance and testing temperature. This can be explained by Holm and Archard’s equation as given below [20, 21]. During the ball-on-disc tests between aluminium and hardened tool steel at elevated temperatures, it is reasonable to assume the ball material (hardened steel) behaves as a rigid material. Therefore, the amount of wear on the disc surface is proportional to the normal load and sliding distance/laps of sliding and inversely proportional to the surface hardness of the disc material, i.e.

$$v = \frac{kWx}{H} \tag{5}$$

where  $v$  is the total volume of wear;  $W$  the applied normal load;  $x$  the total sliding distance and  $H$  the surface hardness of the material. Obviously, the more laps of sliding, the larger amount of wear, or wider and deeper wear track will be. In addition, the hardness of the disc material decreases significantly with increasing temperature, thus wider wear tracks are formed at higher temperatures, as the experiments show (Fig. 5).

#### 4.1.2 Evolution of Contact Area and Mean Contact Pressure

Figure 6 shows the evolution of the apparent contact area during ball-on-disc testing. Due to the removal of the surface material, the wear track becomes wider and the contact area indeed increases with the sliding distance.

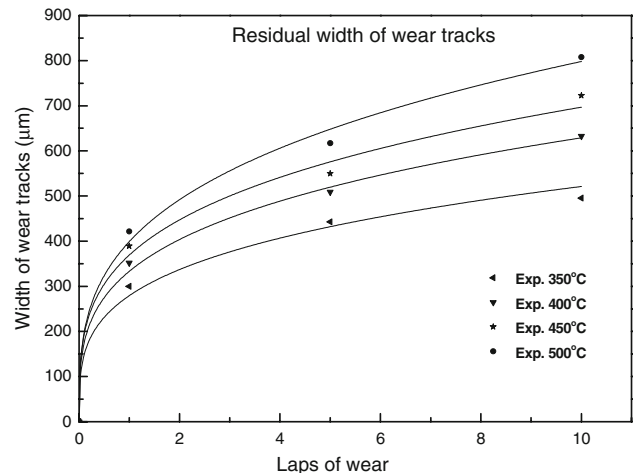


**Fig. 5** Evolution of the width of wear tracks with sliding distance

According to Bowden and Tabor’s classical theory of friction [22], the friction coefficient increases with increasing real contact area. In the present research, aluminium was so soft that severe plastic deformation occurred on the contact interface and the real contact area increases as the apparent contact area increases. Therefore, it is the increasing contact area with the laps of sliding, which results in the increasing friction coefficient as shown in Fig. 4.

Figure 7 shows the evolution of mean contact pressure on the contact interface. As a result of the increasing contact area, the mean contact pressure decreases with increasing sliding distance.

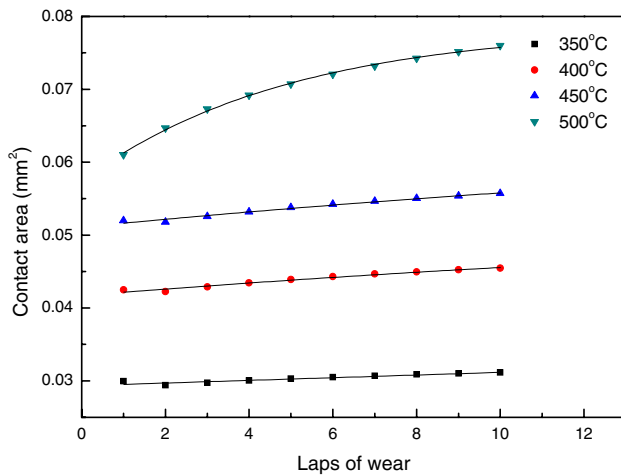


**Fig. 6** Evolution of the apparent contact area with sliding distance

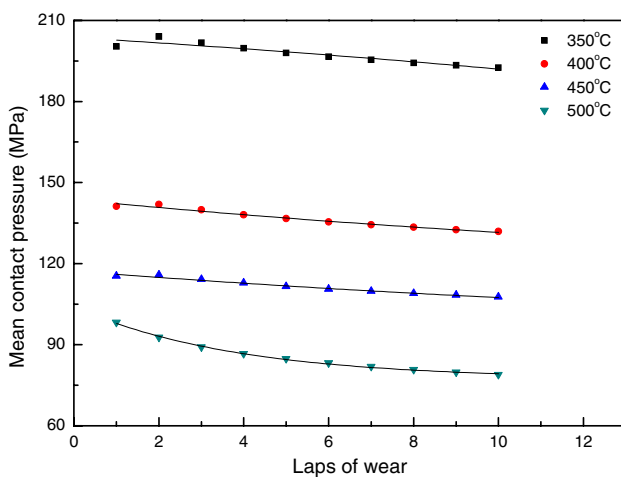


**Fig. 7** Evolution of the mean contact pressure with sliding distance

During the ball-on-disc tests, contact area, mean contact pressure and the friction coefficient varied considerably. Therefore, friction coefficient alone may be insufficient to characterize the friction properties of the mating materials. Friction stress that is the friction force per unit area may be a better option, because it is convenient for the characterization of the friction at the interface involving strong adhesion without specifying the real contact area. It is certainly necessary to understand the evolution of the friction stress further during prolonged pin-on-disc tests.

#### 4.2 Evolution of Shear Friction Stress

Figure 8 shows the evolutions of the calculated shear friction stress at different temperatures and over a sliding distance of 10 laps. It is interesting to see that the shear friction stress starts from a relatively low value, and then becomes quite stable at each of the temperatures, while the

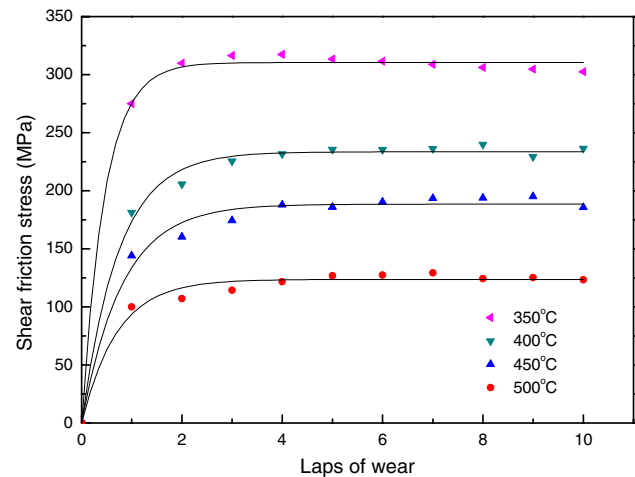


**Fig. 8** Evolution of the shear friction stress with sliding distance

friction coefficient increases considerably (Fig. 4). The low shear friction stress at the initial stage may be due to the oxide layer on the disc and ball surfaces, which tends to lower the adhesion between aluminium and steel [23, 24]. After the initial stage of sliding, the oxide layer may be broken up and metal-to-metal contact occurs, leading to the increases in friction stress. In addition, the severe plastic deformation on the surface material may generate a considerable work-hardening effect [22, 25], which may also lead to the rise of shear friction stress. As can be seen from Fig. 8, the shear friction stress differs markedly at different temperatures, and it is therefore necessary to reveal the influence of temperature on the friction stress.

#### 4.3 Influence of Temperature on the Shear Friction Stress

Figure 9 shows the correlation of the mean shear friction stress with temperature. It has been used as a base to develop a new friction model. The model will be validated by comparing the results from FE simulation and aluminium extrusion experiments in the follow-up research. From Fig. 9, it is clear that the friction stress decreases steadily with increasing temperature, while friction coefficient decreases with increasing temperature. This is consistent with the observations made during the machining process [26] and the results of the friction tests carried out by Bowden and Tabor [22]. It is, however, inconsistent with the results obtained by other researchers from ball-on-disc tests at elevated temperatures [18]. Therefore, more efforts are needed to explain the contradictory results and to reveal the real effect of temperature on friction.

It is commonly understood that the friction force at elevated temperatures stems from the deformation of surface material and the adhesive bonding of the contact joints

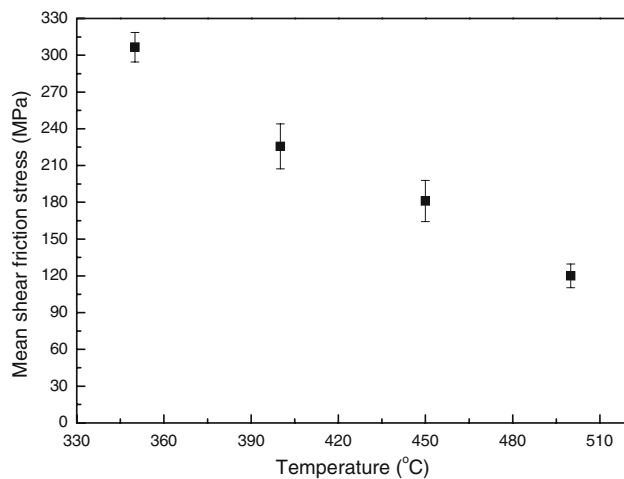


**Fig. 9** Mean shear friction stress as a function of temperature

[22, 27, 28]. As temperature increases, the friction force due to the deformation of the asperities decreases significantly because of the softening effect of the surface material. On the other hand, the adhesive friction plays an increasing important role in determining the overall friction, because the mating materials tend to be more active at elevated temperatures. These phenomena have been investigated in the preceding research. It was found that the adhesive joints stemmed from an intermetallic compound layer generated at the aluminium alloy/steel interface. During the extrusion of AA6063, an Al–Mg–O adhesive layer was observed in the die land area [13], which led to the sticking and chemical wear in the bearing channel of the extrusion die. In the more recent research, the adhesion between 5xxx series aluminium alloys and steel was investigated to simulate the material transfer between workpiece and tooling surface, and strong diffusion bonding was also observed [23, 24]. The composition of the intermetallic compound layer at the aluminium (AA5083)–steel interface was identified as  $(\text{Fe}, \text{Mn})\text{Al}_6$ ,  $\text{Fe}_4\text{Al}_{13}$ ,  $\text{Fe}_2\text{Al}_5$  and  $\text{Mg}_2\text{Si}$  [29]. Therefore, the adhesive strength between the mating materials will be most likely determined by the strength of the intermetallic compound layer, which can be considerably affected by temperature.

At elevated temperatures, the mating materials tend to be more active to generate adhesive bonding between each other, but an increase in friction coefficient may not necessarily appear, because the overall friction coefficient will be determined by many factors, for example, the adhesive strength and real contact area. As temperature increases, the strength of the adhesive joints decreases significantly and thus the friction coefficient tends to decrease. It is, however, important to note that during the high-temperature ball-on-disc tests the area of the contact interface increases with the sliding distance, which may be different

from other types of friction tests. This may increase the number of adhesive joints due to strong adhesion and thus the friction coefficient. Further studies are needed on the physical and chemical tribology of the mating surfaces at elevated temperatures to clarify the correlation between the apparent contact area and friction coefficient under this special circumstance. In addition, the increase of the friction coefficient may be partly caused by hard wear debris generated due to oxidation and entrapped at the interface, because the tests were carried out in the ambient atmosphere and as such the influence of a hard aluminium oxide layer on friction coefficient would be inevitable. The combination of these factors complicates the results of ball-on-disc tests. As a consequence, incomparable results might be obtained from the ball-on-disc tests, as compared to other friction testing methods and friction coefficient alone is most likely insufficient to characterize the interface friction property, when ball-on-disc tests are used. It would be necessary to take the evolution of the contact area/normal pressure into account as well and friction stress might be a better option.

## 5 Conclusions

A series of ball-on-disc tests were carried out at different temperatures. The friction coefficients were found to increase with increasing sliding distance. The individual friction coefficient data could not be utilized directly for FE simulation of the aluminium extrusion process. A model for ball-on-disc tests, developed in the preceding research, was used to reveal the contact between aluminium and tool steel at elevated temperatures. The calculated shear friction stress and mean contact pressure showed that, during the running-in period, the shear friction stress was quite stable, while the friction coefficient increased with increasing sliding distance significantly. Therefore, a fundamental understanding of the evolution of the contact interface must be gained, before the results of ball-on-disc tests can be used as the frictional boundary conditions for FE simulation.

**Open Access** This article is distributed under the terms of the Creative Commons Attribution Noncommercial License which permits any noncommercial use, distribution, and reproduction in any medium, provided the original author(s) and source are credited.

## References

- Fang, G., Zhou, J., Duszczuk, J.: Effect of pocket design on metal flow through single-bearing extrusion dies to produce a thin-walled aluminium profile. *J. Mater. Process. Technol.* **199**, 91–101 (2008)

2. Liu, G., Zhou, J., Duszczyc, J.: FE analysis of metal flow and weld seam formation in a porthole die during the extrusion of a magnesium alloy into a square tube and the effect of ram speed on weld strength. *J. Mater. Process. Technol.* **200**, 185–198 (2008)
3. Yang, D.Y., Park, K., Kang, Y.S.: Integrated finite element simulation for the hot extrusion of complicated Al alloy profiles. *J. Mater. Process. Technol.* **111**, 25–30 (2001)
4. Sheppard, T.: *Extrusion of Aluminium Alloys*. Kluwer Academic Press, Dordrecht (1999)
5. Chanda, T., Zhou, J., Kowalski, L., Duszczyc, J.: 3D FEM simulation of the thermal events during AA6061 aluminium extrusion. *Scr. Mater.* **41**(2), 195–202 (1999)
6. Wagener, H.W., Wolf, J.: Coefficient of friction in cold extrusion. *J. Mater. Process. Technol.* **44**, 283–291 (1994)
7. Tan, X., Bay, N., Zhang, W.: Friction measurement and modelling in forward rod extrusion tests. *Proc. Inst. Mech. Eng. J* **217**, 71–82 (2003)
8. Bakhshi-Jooybari, M.: A theoretical and experimental study of friction in metal forming by the use of the forward extrusion process. *J. Mater. Process. Technol.* **125–126**, 369–374 (2002)
9. Flitta, I., Sheppard, T.: Nature of friction in extrusion process and its effect on material flow. *Mater. Sci. Technol.* **19**, 837–846 (2003)
10. Schikorra, M., Donati, L., Tomesani, L., Kleiner, M.: The role of friction in the extrusion of AA6060 aluminum alloy, process analysis and monitoring. *J. Mater. Process. Technol.* **191**, 288–292 (2007)
11. Tverlid, S.: Modelling of friction in the bearing channel of dies for extrusion of aluminium sections. PhD Thesis, Norwegian University of Science and Technology, Trondheim (1997)
12. Welo, T., Abtahi, S., Skauvik, I., Støren, S., Melander, M., Tjøtta, S.: Friction in the bearing channel of aluminium extrusion dies. In: *Proceedings of 15th Riso International Symposium on Materials Science*, Roskilde, Denmark, pp. 615–620 (1994)
13. Thedja, W.W., Müller, K.B., Ruppin D.: Tribomechanical process on the die land area during extrusion of AA6063 alloy. In: *Proceedings of the 5th International Aluminium Extrusion Technology Seminar*, vol. II, pp. 467–474 (1992)
14. Bonnet, C., Valiorgue, F., Rech, J., Claudin, C., Hamdi, H., Bergheau, J.M., Gilles, P.: Identification of a friction model—application to the context of dry cutting of an AISI 316L austenitic stainless steel with a TiN coated carbide tool. *Int. J. Mach. Tools Manuf.* **48**, 1211–1223 (2008)
15. Behrens, A., Schafstall, H.: 2D and 3D simulation of complex multistage forging processes by use of adaptive friction coefficient. *J. Mater. Process. Technol.* **80**, 298–303 (1998)
16. Björk, T., Bergström, J., Hogmark, S.: Tribological simulation of aluminium hot extrusion. *Wear* **224**, 216–225 (1999)
17. Wang, L., He, Y., Zhou, J., Duszczyc, J.: Modelling of plowing and shear friction coefficients during high-temperature ball-on-disc tests. *Tribol. Int.* **42**, 15–22 (2009)
18. Ranganatha, S., Kailas, S.V., Støren, S., Srivatsan, T.S.: Role of temperature on sliding response of aluminum on steel of a hot extrusion. *Mater. Manuf. Process.* **23**, 29–36 (2008)
19. Tayebi, N., Conry, T.F., Polycarpou, A.A.: Determination of hardness from nanoscratch experiments: corrections for interfacial shear stress and elastic recovery. *J. Mater. Res.* **18**, 2150–2162 (2003)
20. Holm, R.: *Electric Contacts*. Almqvist and Wiksells, Stockholm (1946)
21. Archard, J.F.: Contact and rubbing of the flat surfaces. *J. Appl. Phys.* **24**, 981–988 (1953)
22. Bowden, F.P., Tabor, D.: *The Friction and Lubrication of Solids*. Part I. Clarendon Press, Oxford (1950)
23. Riahi, A.R., Alpas, A.T.: Adhesion of AA5182 aluminum sheet to DLC and TiN coatings at 25 degrees C and 420 degrees C. *Surf. Coat. Technol.* **202**, 1055–1061 (2007)
24. Riahi, A.R., Edrissy, A., Alpas, A.T.: Effect of magnesium content on the high temperature adhesion of Al–Mg alloys to steel surfaces. *Surf. Coat. Technol.* **203**, 2030–2035 (2009)
25. Hutchings, I.M.: *Tribology: Friction and Wear of Engineering Materials*. Edward Arnold, London (1992)
26. Moufki, A., Molinari, A., Dudzinski, D.: Modelling of orthogonal cutting with a temperature dependent friction law. *J. Mech. Phys. Solids* **46**, 2103–2138 (1998)
27. Suh, N.P.: *Tribophysics*. Prentice Hall, Englewood Cliffs, NJ (1986)
28. Bhushan, B.: *Introduction to Tribology*. Wiley, New York (2002)
29. Yamamoto, N., Takahashi, M., Ikeuchi, K., Aritoshi, M.: Interfacial layer in friction-bonded joint of low carbon steel to Al–Mg alloy (AA5083) and its influence on bond strength. *Mater. Trans.* **45**, 296–299 (2004)